

Reaction kinetics of the $\text{MmNi}_{4.5}\text{Al}_{0.5}\text{-H}$ system

X.-L. Wang and S. Suda

Department of Chemical Engineering, Kogakuin University, 2665-1, Nakano-machi, Hachioji-shi, 192 Tokyo (Japan)

(Received July 12, 1991; in final form November 6, 1991)

Abstract

The hydriding and dehydriding reaction kinetics of the aluminum-substituted mischmetal–nickel hydride were studied. The experiments were carried out by a step-wise method in the α and $\alpha + \beta$ phase regions in the temperature range from 303.2 to 333.2 K. The effects of the phase change on reaction characteristics were examined. The reaction was found to proceed differently between different phase regions for both the hydriding and dehydriding processes. The reaction order, rate constant, and apparent activation energy change with phase regions under isothermal conditions. However, those parameters are kept constant within a given phase region.

1. Introduction

Mischmetal (Mm) is a mixture of rare earth elements. It has been expected that Mm–Ni hydrides would be employed for energy conversion systems such as rechargeable batteries, heat pumps, power generators, compressors etc. because of their rapid kinetics, large hydrogen storage capacity and relatively low cost [1]. These Mm-based hydriding materials have been successfully used to make a rechargeable battery which is commercially obtainable [2, 3]. However, these hydride systems are considered to be the most complicated systems for both experimental and theoretical analyses because of their multicomponents, high plateau pressure, large hysteresis and sloping plateau.

Many studies on the reaction kinetics of metal hydrides have been carried out over the past several years. However, there is little agreement among the reported experimental data because of the difficulties in performing experiments under isothermal conditions. It is recognized that in previous studies [4, 5], heat transfer has restricted the rate of hydrogen transfer.

A method has been developed for the reduction of thermal effects caused by reaction heat, and for the detailed determination of reaction kinetics; this method involves the design of a double-walled reactor [6] and the introduction of a step-wise measuring method [7, 8]. The reactor is constructed as a double-walled structure in which the space between inner and outer tubes as a sample holder is kept at 0.5 mm. This reactor provides a very high heat transfer rate with a large heat transfer area and thin sample layer. By applying the step-wise method, determination of the reaction kinetics in each

phase region, *i.e.* in the α , $\alpha+\beta$ and β phase regions, can be performed independently. The minimal involvement of reaction heat makes it possible to eliminate thermal effects at the lowest level possible.

In this paper the kinetics of the hydriding and dehydriding reactions for the $\text{MmNi}_{4.5}\text{Al}_{0.5}\text{-H}$ system were determined in detail using the proposed experimental method. The reaction was performed in both the α and $\alpha+\beta$ phase regions to examine the effects of phase changes. By means of the rate equations so established the reaction order, rate constant and apparent activation energy were estimated. The change of those parameters with phase regions was examined.

2. Experimental details

Experiments were performed by a step-wise method [7, 8] under isothermal, isochoric, and variable pressure conditions. A detailed description of the apparatus used for the present kinetic studies is given in ref. 6. The experiments were carried out using a double-walled reactor which provides a 0.5 mm annular space as a sample holder. The reactor was immersed in a thermostat bath and water of a given temperature was pumped through the inner tube to secure high heat transfer. The quantities of absorbed or desorbed hydrogen were measured by a volumetric method. The data were taken in the temperature range from 303.2 to 333.2 K after more than 40 hydriding-dehydriding repeating cycles. The pressure change was measured at 0.2 s intervals for 2 min after starting each experimental run and the data were recorded on a tape cartridge. A sample of 5 g of $\text{MmNi}_{4.5}\text{Al}_{0.5}$ was used and the composition of the mischmetal was as shown in Table 1.

3. Rate equations

In past studies rate equations for both the hydriding and dehydriding reactions have been derived from the reaction characteristics of the metal hydride systems [7, 8]

$$\text{Hydriding: } dc/dt = k_h (P/P_{eh})^\alpha [1 - (P_f/P)^\alpha (C/C_f)^b] \quad (1)$$

$$k_h = A e^{-E_h/RT}$$

$$\text{Dehydriding: } dc/dt = k_d (C^b/P_{ed}^\alpha) [1 - (C_f/C)^b (P/P_f)^\alpha] \quad (2)$$

$$k_d = A' e^{-E_d/RT}$$

TABLE 1

Composition of mischmetal

Mm	La	Ce	Nd	Pr	Sm	Al	Mg
Wt.%	18.43	57.25	14.51	7.00	0.70	<0.01	<0.03

In the above rate equations, the constants, k_h and k_d are the rate constants, the constants a and b are the reaction orders, P is the hydrogen pressure at a given time interval during the reaction, P_f is the final equilibrium pressure for a given experimental run, P_e is the plateau pressure, C and C_f are the hydrogen concentrations, H/M , after a given reaction time interval and in the final equilibrium condition. The subscripts, h and d, represent the hydriding and dehydriding processes.

The rate constants are kept constant regardless of hydrogen pressure and concentration under isothermal conditions if there is no phase change from the α phase region to the $\alpha + \beta$ phase region or from the $\alpha + \beta$ phase region to the β phase region. Straight-line relationships can be expected when reaction rates, dc/dt , are plotted against $f(P, C)$ of the right-hand side of the equation. The apparent rate constant can be estimated from the slopes of the straight lines.

4. Results and discussion

4.1. Equilibrium properties

The P - C - T equilibrium properties of the $\text{MmNi}_{4.5}\text{Al}_{0.5}$ -H system were examined. Figures 1 and 2 illustrate the hydriding and dehydriding P - C - T relations obtained under several isothermal conditions. The plateau pressure, P_e , and the hysteresis are listed in Table 2, where the plateau pressure is defined as the average pressure in the plateau region at each P - C isotherm (it is the value at the center of the plateau region for each isotherm). In this MH system there is a comparatively wide plateau region accompanied

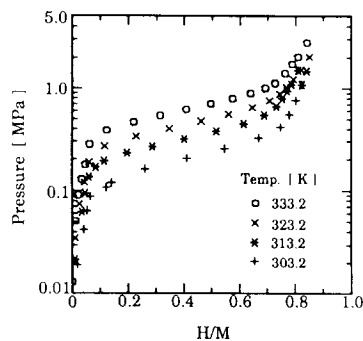
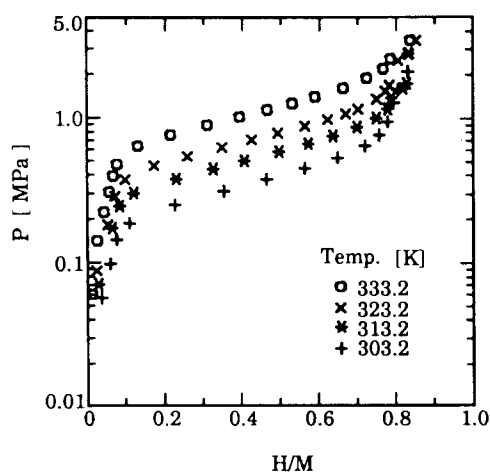


Fig. 1. The P - C isotherms of hydriding reaction of $\text{MmNi}_{4.5}\text{Al}_{0.5}$ -H system at 303.2–333.2 K.

Fig. 2. The P - C isotherms of dehydriding reaction of $\text{MmNi}_{4.5}\text{Al}_{0.5}$ -H system at 303.2–333.2 K.

TABLE 2

Hydriding and dehydriding plateau pressures at several temperatures

Temperature (K)	303.2	313.2	323.2	333.2
Plateau pressure (MPa)				
P_{eh}	0.34	0.50	0.70	1.05
P_{ed}	0.24	0.35	0.50	0.70
ΔP	0.10	0.15	0.20	0.25

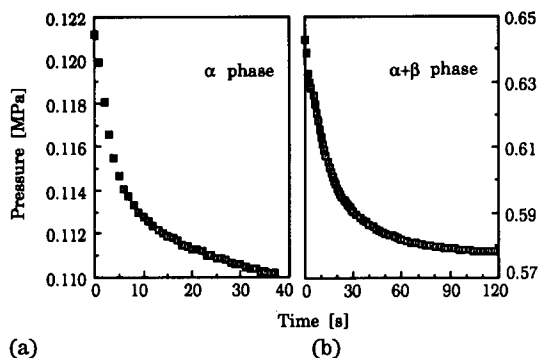


Fig. 3. Variations of the hydrogen pressure for the hydriding reaction in the α and $\alpha + \beta$ phase regions at 313.2 K: (a) α phase: starting pressure and concentration $P_i = 0.121$ MPa, $C_i = 0.032$ H/M, equilibrium pressure and concentration $P_f = 0.108$ MPa, $C_f = 0.050$ H/M; (b) $\alpha + \beta$ phase: starting pressure and concentration $P_i = 0.643$ MPa, $C_i = 0.408$ H/M, equilibrium pressure and concentration $P_f = 0.576$ MPa, $C_f = 0.498$ H/M.

with strong slopes. High plateau pressure and large hysteresis were observed. In comparison with the results of the $\text{LaNi}_{5-x}\text{Al}_x$ hydride systems [9], the Mm compound shows higher and more sloping plateaux, and larger hysteresis. The change in thermodynamic properties might result in some differences in the kinetic characteristics.

4.2. Hydriding reactions in the α and $\alpha + \beta$ phase regions

Hydriding reactions were performed by giving step-wise changes in hydrogen concentration in the temperature range between 303.2 and 333.2 K. The typical variations of the pressure against time elapsed are shown in Fig. 3 where the data were taken at 313.2 K in the α and $\alpha + \beta$ phase regions.

The analysis of experimental data to determine the reaction order and the value of rate constant can be carried out according to the following method. When the reaction order is assumed, a straight-line relationship can be obtained by plotting reaction rates, (dc/dt) , against $(P/P_{eh})^a [1 - (P_f/P)^a (C/C_f)^b]$ by means of the rate equation. This straight relationship can be verified by plotting the experimental data. If the experimental data can be fitted to the equation, the value of the reaction order and the rate constant can be obtained. For this $\text{MmNi}_{4.5}\text{Al}_{0.5}$ hydride system, the reaction order a was

determined as 1.0 and 1.5 for the α and $\alpha+\beta$ phase regions respectively by fitting the experimental data to eqn. 1. The reaction order b was determined as 1.0 for both the α and $\alpha+\beta$ phase regions. Figure 4 illustrates the reaction rates as a function of $(P/P_{eh})^a[1-(P_f/P)^a(C/C_f)^b]$ at various initial hydrogen concentrations at 313.2 K in the α phase region. Excellent straight lines were obtained and the rate constants were calculated from the slopes of those straight lines. Data obtained at other isothermal conditions in the α phase region gave analogous profiles. Those results are shown in Fig. 5. Regarding the reaction in the $\alpha+\beta$ phase region, the results obtained at different hydrogen concentrations and temperatures are shown in Figs. 6 and 7. The rate constants obtained at different hydrogen concentrations are listed in Tables 3 and 4 for the α and $\alpha+\beta$ phase regions respectively. It was found that values of the rate constants remained constant regardless of the change of hydrogen concentration in a given phase region. The Arrhenius plot of rate constants vs. $1/T$ is presented in Fig. 8 for the α and $\alpha+\beta$ phase regions. The apparent activation energies were evaluated as 22.75 and 22.18 kJ (mol⁻¹ H₂) for the α and $\alpha+\beta$ phase regions respectively.

4.3. Dehydrating reactions in the α and $\alpha+\beta$ phase regions

The dehydrating reaction kinetics was determined in the α and $\alpha+\beta$ phase regions at temperature range between 303.2 and 333.2 K. The reaction orders, a and b , were determined as 1 and 1.5 by fitting the experimental data to the rate equation, respectively. Figure 9 illustrates the reaction rates obtained at 313.2 K against $(C^{1.5}/P_{ed})[1-(C_f/C)^{1.5}(P/P_f)]$ for the reactions in the α phase region. A similar profile was observed for the reactions at various isothermal conditions in the α phase region. The results are shown in Fig. 10 where the reactions started from the hydrogen concentration of 0.05 H/M and terminated at 0.04 H/M. By plotting dehydrating reaction

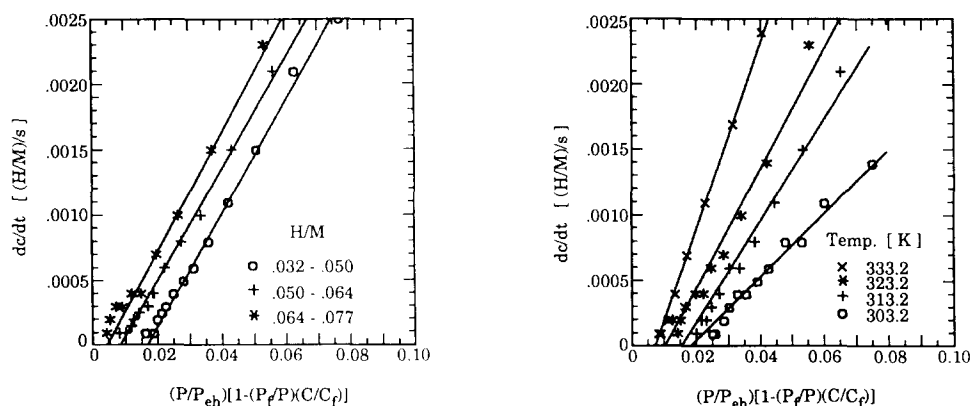


Fig. 4. Hydriding reaction rates vs. $(P/P_{eh})[1-(P_f/P)(C/C_f)]$ at different hydrogen concentrations in the α phase region at 313.2 K.

Fig. 5. Hydriding reaction rates vs. $(P/P_{eh})[1-(P_f/P)(C/C_f)]$ at different temperatures in the α phase region.

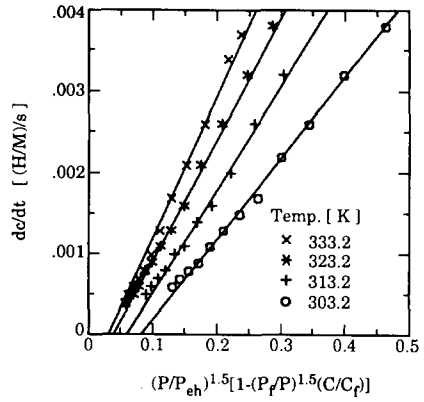
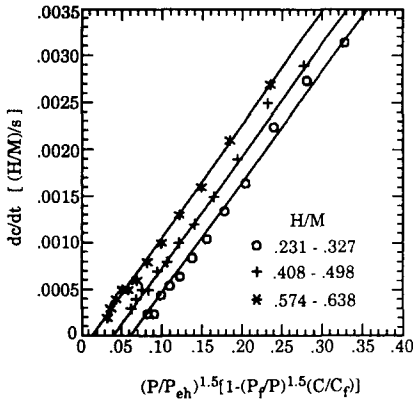


Fig. 6. Hydriding reaction rates vs. $(P/P_{eh})^{1.5}[1-(P_f/P)^{1.5}(C/C_f)]$ at different hydrogen concentrations in the $\alpha + \beta$ phase region at 313.2 K.

Fig. 7. Hydriding reaction rates vs. $(P/P_{eh})^{1.5}[1-(P_f/P)^{1.5}(C/C_f)]$ at different temperatures in the $\alpha + \beta$ phase region.

TABLE 3

Rate constants of hydriding reaction at various hydrogen concentrations in the α phase region

Temperature (K)	Hydrogen concentration (H/M)	Rate constants (H/M s ⁻¹ × 10 ⁻²)
303.2	0.034–0.048	2.34
	0.048–0.059	2.58
	0.059–0.067	2.63
	0.067–0.076	2.92
313.2	0.018–0.032	3.96
	0.032–0.050	3.93
	0.050–0.064	3.96
	0.064–0.077	4.16
323.2	0.020–0.032	4.64
	0.032–0.050	4.59
	0.050–0.063	4.79
	0.063–0.074	4.51
333.2	0.019–0.031	7.10
	0.031–0.061	5.81
	0.061–0.071	6.30
	0.071–0.081	5.37

rates against $(C^{1.5}/P_{ed})[1-(C_f/C)^{1.5}(P/P_f)]$, excellent straight lines were obtained as expected from eqn. (2). The rate constants were calculated from the slopes of those straight lines, and the results are summarized in Table 5.

For the dehydriding reaction in the $\alpha + \beta$ phase region, Fig. 11 illustrates the results obtained at 313.2 K for various initial hydrogen concentrations.

TABLE 4

Rate constants of hydriding reaction at various hydrogen concentrations in the $\alpha+\beta$ phase region

Temperature (K)	Hydrogen concentration (H/M)	Rate constants (H/M s ⁻¹ × 10 ⁻²)
303.2	0.112–0.228	0.916
	0.228–0.355	1.060
	0.355–0.466	0.924
	0.466–0.565	0.863
	0.565–0.650	0.820
	0.650–0.721	0.820
	0.721–0.758	0.756
313.2	0.758–0.780	0.871
	0.122–0.231	1.22
	0.231–0.327	1.19
	0.327–0.408	1.20
	0.408–0.498	1.23
	0.498–0.574	1.17
	0.574–0.638	1.14
323.2	0.638–0.700	1.15
	0.176–0.262	1.43
	0.262–0.352	1.62
	0.352–0.429	1.61
	0.429–0.497	1.61
	0.497–0.567	1.63
	0.567–0.626	1.54
333.2	0.626–0.673	1.47
	0.218–0.313	1.74
	0.313–0.397	1.98
	0.397–0.469	2.00
	0.469–0.534	1.95
	0.534–0.593	2.06
	0.593–0.666	1.85
0.666–0.727	2.04	
	0.727–0.770	1.88

By fitting the experimental data to eqn. (2), the reaction orders a and b were both evaluated to be 1. Linear relationships were obtained with considerable accuracy. Figure 12 is an illustration showing the linearity of the plots obtained at the temperature range between 303.2 and 333.2 K, where reactions started at 0.5 H/M and terminated at 0.4 H/M. Rate constants were obtained from those slopes, and the values are listed in Table 6.

The Arrhenius plots of the rate constants *vs.* $1/T$ are shown in Fig. 13 to clarify the temperature dependence of the rate constants. The apparent activation energies for the dehydriding reaction in the α and $\alpha+\beta$ phase regions were evaluated to be 68.1 and 60.2 kJ (mol⁻¹ H₂) respectively.

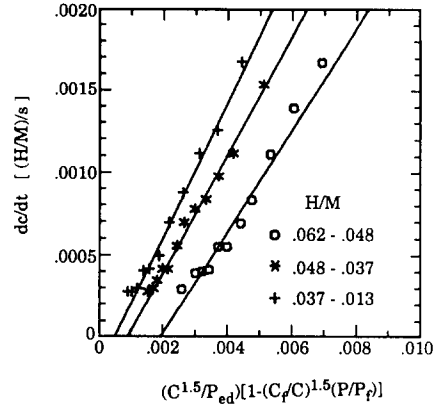
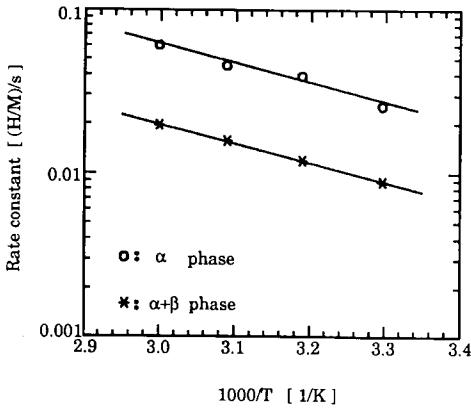


Fig. 8. Arrhenius plots of hydriding reaction for the α and $\alpha+\beta$ phase regions.

Fig. 9. Dehydriding reaction rates vs. $(C^{1.5}/P_{ed})[1-(C_t/C)^{1.5}(P/P_t)]$ at different hydrogen concentrations in the α phase region at 313.2 K.

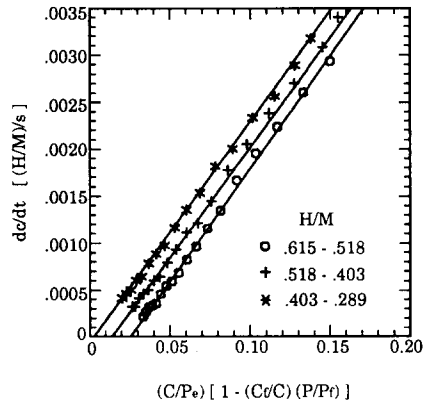
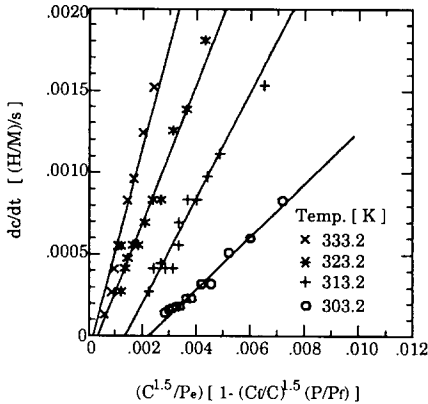


Fig. 10. Dehydriding reaction rates vs. $(C^{1.5}/P_{ed})[1-(C_t/C)^{1.5}(P/P_t)]$ at different temperatures in the α phase region.

Fig. 11. Dehydriding reaction rates vs. $(C/P_{ed})[1-(C_t/C)(P/P_t)]$ at different hydrogen concentrations in the $\alpha+\beta$ phase region at 313.2 K.

4.4. Discussion

In summary, the rate constants, k_h and k_d , the reaction orders, a and b , and the apparent activation energy obtained in this experiment are summarized in Table 7. It is clearly shown that those parameters change with phase regions under isothermal conditions. However, those are kept constant within a given phase region. It was also observed in this experiment that the initial reaction rates in the α and β phase regions are much faster than that in the $\alpha+\beta$ phase region. Those observations indicate that the reaction proceeds differently for each phase region. Some recent papers have reported the dependency of the rate constant on hydrogen pressure [10] and hydrogen concentration [11] for the hydriding reactions (but no reported

TABLE 5

The rate constants of dehydrating reaction at various hydrogen concentrations in the α phase region

Temperature (K)	Hydrogen concentration (H/M)	Rate constants (MPa s ⁻¹ × 10 ⁻¹)
303.2	0.067–0.056	0.34
	0.056–0.044	0.49
	0.044–0.021	0.41
313.2	0.086–0.062	1.28
	0.062–0.048	1.30
	0.048–0.037	1.13
323.2	0.064–0.048	2.43
	0.048–0.030	2.01
	0.030–0.016	1.72
333.2	0.066–0.050	5.36
	0.050–0.038	5.06
	0.038–0.025	3.84
	0.025–0.016	5.31

dehydrating data to be referred). It is thought that those data might contain the combined effects which are caused by the reactions across over the different phase regions. In those cases the reaction did not stay within a single phase but ran over from the α phase region to the β phase region *via* the $\alpha + \beta$ phase region. The calculated rate constant might be the values averaged in three different phase regions.

Regarding the reaction order, it was observed that the reaction order, α , of the $\text{MmNi}_{4.5}\text{Al}_{0.5}$ is smaller than that of the $\text{LaNi}_{4.7}\text{Al}_{0.3}$ [7, 8]. It is considered that the change in reaction order might be caused by a change in the thermodynamic properties and/or the reaction mechanisms. As expressed in eqns. (1) and (2), the reaction rate is a function of pressure (P) and concentration (H/M), especially of the plateau pressure for the MH systems. The high plateau pressure may be the most influential factor in lowering the reaction order. However, much more information would be necessary to give an exact explanation of the significance of the change in reaction order.

Based on the results obtained in different phase regions, it is understood that several rate-controlling steps exist during the hydriding and dehydrating reactions when the reaction proceeds from the α to the β phase regions. The rate-controlling step might change with phase regions. In past studies the rate controlling steps for the hydriding [8] and dehydrating [7] reactions of $\text{LaNi}_{4.7}\text{Al}_{0.3}\text{-H}$ system have been hypothesized. It is considered that the $\text{MmNi}_{4.5}\text{Al}_{0.5}\text{-H}$ system has the same rate controlling steps as the $\text{LaNi}_{4.7}\text{Al}_{0.3}\text{-H}$ system on the basis of the similar kinetic tendency between each phase region. The rate controlling steps for the hydriding reaction are the surface process in the α phase region, the nucleation and growth of hydride in the $\alpha + \beta$ phase region and the diffusion of hydrogen atoms through the hydride

TABLE 6

The rate constants of dehydrating reaction at various hydrogen concentrations in the $\alpha + \beta$ phase region

Temperature (K)	Hydrogen concentration (H/M)	Rate constants (MPa s ⁻¹ × 10 ⁻²)
303.2	0.748–0.670	0.487
	0.670–0.547	0.437
	0.547–0.412	0.401
	0.412–0.262	0.384
	0.262–0.143	0.403
313.2	0.689–0.615	0.889
	0.615–0.518	0.833
	0.518–0.403	0.812
	0.403–0.288	0.788
	0.288–0.197	0.735
	0.197–0.116	0.812
323.2	0.710–0.649	1.925
	0.649–0.563	1.895
	0.563–0.465	1.905
	0.465–0.351	1.845
	0.351–0.232	1.845
	0.232–0.120	2.065
333.2	0.730–0.695	3.892
	0.695–0.643	3.451
	0.643–0.578	3.262
	0.578–0.500	3.262
	0.500–0.412	3.542
	0.412–0.318	3.430
	0.318–0.223	3.605

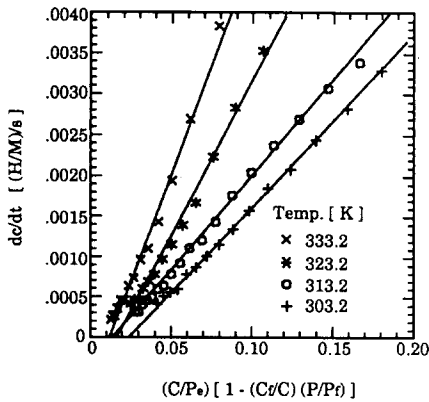


Fig. 12. Dehydrating reaction rates vs. $(C/P_e)[1 - (C_t/C)(P/P_t)]$ at different temperatures in the $\alpha + \beta$ phase region.

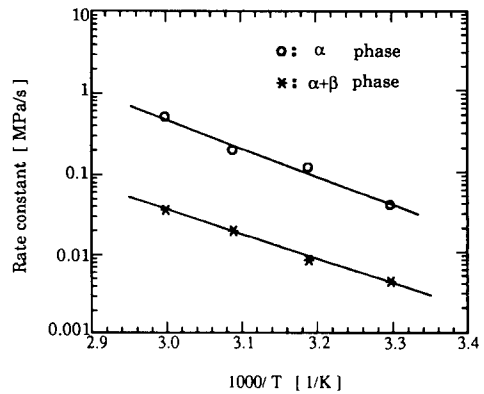


Fig. 13. Arrhenius plots of dehydrating reactions for the α and $\alpha + \beta$ phase regions.

TABLE 7

Some parameters obtained in the α and the $\alpha + \beta$ phase regions for the $\text{MmNi}_{4.5}\text{Al}_{0.5}\text{-H}$ system^a

	Hydriding		Dehydriding	
	α phase	$\alpha + \beta$ phase	α phase	$\alpha + \beta$ phase
a	1	1.5	1	1
b	1	1	1.5	1
k	0.040	0.012	0.124	0.0081
E	22.8	22.2	68.1	60.2

^a k is the average value at 313.2 K.

layer in the β phase region. In the case of dehydriding reaction, rate controlling steps are the diffusion of hydrogen atoms through the hydride layer, the decomposition of hydride and the surface process with corresponding to the β , the $\alpha + \beta$ and the α phase regions.

5. Conclusions

The reactions were found to proceed quite differently for each phase region. Reaction rates in the α and the β phase regions are much faster than those in the $\alpha + \beta$ phase region. The reaction order, rate constant, apparent activation energy and rate-controlling steps change with phase regions. However, those parameters are kept constant within a given phase region.

Acknowledgment

We wish to thank Mr. T. Kai, an undergraduate student, for his experimental assistance.

References

- 1 S. Suda and Y. Komazaki, *J. Less-Common Met.*, 89 (1983) 127.
- 2 T. Sakai, T. Hazama, H. Miyamura, N. Kuriyama, A. Kato and H. Ishikawa, *J. Less-Common Met.*, 172-174 (1991) 1175.
- 3 K. Inoue, T. Matsumoto, S. Kameoka and N. Furukawa, *Sanyo Technical Review*, 20(3) (1988) 86.
- 4 A. J. Goudy and R. A. Wallingford, *J. Less-Common Met.*, 99 (1984) 249.
- 5 X.-L. Wang and S. Suda, *Int. J. Hydrogen Energy*, 15 (8) (1990) 569.
- 6 S. Suda, N. Kobayashi and K. Yoshida, *J. Less-Common Met.*, 73 (1980) 119.

- 7 X.-L. Wang and S. Suda, *J. Less-Common Met.*, 159 (1990) 83.
- 8 X.-L. Wang and S. Suda, *J. Less-Common Met.*, 159 (1990) 109.
- 9 X.-L. Wang and S. Suda, submitted to the International Conference on Rare Earths '92 in Kyoto, Japan.
- 10 C. M. Stander, *J. Inorg. Nucl. Chem.*, 39 (1977) 221.
- 11 J. S. Han and J. Y. Lee, *J. Less-Common Met.*, 131 (1987) 109.